Trop J Nat Prod Res, December 2025; 9(12): 6249 – 6257

ISSN 2616-0684 (Print)
ISSN 2616-0692 (Electronic)

Tropical Journal of Natural Product Research

Available online at https://www.tjnpr.org

Original Research Article

Potential Cytotoxic Isolates of *Spigelia anthelmia* Linn. against T47D and WiDr Cancer Cells

Muhammad Taupik[1]*, Nanang Fakhruddin[2], Mohamad A. Mustapa[3], Endah N. Djuwarno[4], Qamar U. Ahmed[5]

[1] *Department of Pharmacy, Faculty of Sports and Health, Gorontalo State University, Gorontalo 96211, Indonesia.*
[2] *Department of Pharmaceutical Biology, Faculty of Pharmacy, Gadjah Mada University, Yogyakarta, Indonesia*
[3] *Department of Pharmacy, Faculty of Sports and Health, Gorontalo State University, Gorontalo 96211, Indonesia.*
[4] *Department of Pharmacy, Faculty of Sports and Health, Gorontalo State University, Gorontalo 96211, Indonesia.*
[5] *Department of Pharmaceutical Chemistry, Faculty of Pharmacy, International Islamic University Malaysia, Kuantan, Malaysia*

ARTICLE INFO

Article history:
Received 17 September 2025
Revised 02 December 2025
Accepted 04 December 2025
Published online 01 January 2026

ABSTRACT

Natural products continue to provide valuable leads for anticancer drug discovery, yet limited studies have addressed the bioactive constituents of *Spigelia anthelmia* Linn. This research aimed to isolate and characterize cytotoxic metabolites of *S. anthelmia* using a bioassay-guided isolation approach. Sequential extraction, vacuum liquid chromatography (VLC), and preparative thin-layer chromatography (PTLC) yielded a semi-purified fraction designated as Isolate A. Cytotoxicity was evaluated against T47D breast cancer and WiDr colon cancer cells using the MTT assay. Isolate A significantly reduced cell viability in a dose-dependent manner (ANOVA, $p < 0.05$), with IC_{50} values of 166.92 ± 5.10 µg/mL (T47D) and 245.24 ± 6.25 µg/mL (WiDr), whereas doxorubicin exhibited IC_{50} values of 40.05 ± 2.30 µg/mL and 3.57 ± 0.45 µg/mL, respectively. Flow cytometry with Annexin V–FITC/PI staining revealed a visible shift of cell populations toward early and late apoptotic quadrants, indicating apoptosis as the predominant mechanism of cell death. Spectroscopic characterization by FTIR, LC–MS, and NMR suggested that Isolate A is a phenolic/alkaloid-type compound (m/z 218 $[M+H]^+$) containing hydroxyl, carbonyl, and heteroaromatic groups. Collectively, these findings demonstrate that *S. anthelmia* contains apoptosis-inducing metabolites with measurable cytotoxicity, supporting its potential as a natural source of anticancer leads and warranting further purification and mechanistic investigation. To our knowledge, this is the first study to combine bioassay-guided isolation, apoptosis profiling, and spectroscopic characterisation of *S. anthelmia* metabolites in T47D and WiDr cancer cells.

Keywords: Bioassay-guided isolation; Cytotoxicity; Apoptosis; Phenolic alkaloids; *Spigelia anthelmia*; Spectroscopic characterization

Introduction

Cancer remains a major cause of global morbidity and mortality, driving continuous exploration of novel therapeutic agents from natural sources.[1,2] Medicinal plants are particularly important because of their structural diversity and bioactive metabolites, many of which serve as lead compounds for anticancer drug development.[3] Several plant-derived secondary metabolites, including alkaloids, phenolics, and terpenoids, have demonstrated the ability to induce apoptosis and inhibit cancer cell proliferation through modulation of cell-cycle checkpoints, mitochondrial pathways, and oxidative-stress responses.[4,5] Bioassay-guided fractionation has proven particularly effective in discovering new cytotoxic agents. For instance, six novel elatostemanosides (I–VI) were recently isolated from *Elatostema tenuicaudatum*, exhibiting IC_{50} values of 18.2–57.6 µM against HepG2 and HCC1806 cells, with apoptosis induction via modulation of the Bax/Bcl-2 ratio.[6]

*Corresponding author. E mail: muhtaupik@ung.ac.id
Tel: +6281547458537

Citation: Taupik M, Fakhruddin N, Mustapa MA, Djuwarno EN, Ahmed QU. Potential Cytotoxic Isolates of *Spigelia anthelmia* Linn. against T47D and WiDr Cancer Cells. Trop J Nat Prod Res. 2025; 9(12): 6249 – 6257 https://doi.org/10.26538/tjnpr/v9i12.44

Official Journal of Natural Product Research Group, Faculty of Pharmacy, University of Benin, Benin City, Nigeria

Similarly, the flowers of *Aquilaria sinensis* yielded active benzophenone glycosides (aquilasides B and C) that showed moderate cytotoxicity against SK-MEL cells (IC_{50} ~12–17 µM), while other constituents demonstrated selective activity in lung cancer lines versus normal bronchial cells.[7] Agarwood derived from *A. sinensis* has also produced new guaiane sesquiterpenes and cucurbitacins with pronounced cytotoxic effects and apoptosis induction in human breast cancer cells.[8] *Spigelia anthelmia* Linn. (Loganiaceae) is a tropical herb widely distributed in South America, Africa, and Asia. Traditionally employed as an anthelmintic, this plant is also classified among toxic herbs, reflecting its rich repertoire of potent secondary metabolites.[9,10] Phytochemical investigations have revealed the presence of spiganthine alkaloids, flavonoids such as 3,7-dihydroxy-3′,4′-dimethoxyflavone, and diterpenoids including ryanodol, all of which may underlie its pharmacological and toxicological activities.[11,12] More recent studies have expanded its profile, reporting antioxidant activity in methanolic fractions[13] and preliminary cytotoxic screening in diverse cell lines.[14,15] In Indonesia, preliminary screening showed that *S. anthelmia* possessed very high lethality (94%) in the brine shrimp lethality test (BST) among eleven coastal plants from Bantul, Yogyakarta, and subsequent work confirmed its antiparasitic activity against *Haemonchus contortus* larvae and gastrointestinal nematodes in sheep.[16,17] Despite these findings, systematic investigations that link *S. anthelmia* metabolites with cytotoxic effects in human cancer cells—accompanied by apoptosis assays and spectroscopic characterization of the active constituents—remain scarce. Considering its dual identity as both medicinal and toxic, this study was designed to explore the cytotoxic potential of *S. anthelmia* through a bioassay-guided isolation approach.

Extracts and fractions were screened using BST, followed by cytotoxic evaluation against T47D breast cancer and WiDr colon cancer cell lines using the MTT assay. The most active isolate was subsequently assessed for apoptosis-inducing activity by flow cytometry and structurally characterized using Fourier-transform infrared (FTIR) spectroscopy, liquid chromatography–mass spectrometry (LC–MS), and nuclear magnetic resonance (NMR). In this context, the present work provides the first integrated assessment of bioassay-guided isolation, detailed spectroscopic analysis, and Annexin V–FITC/PI apoptosis profiling of *S. anthelmia* metabolites in T47D and WiDr cells, thereby highlighting this species as a promising natural source for anticancer lead compounds.

Materials and Methods

Plant Material and Authentication

Fresh specimens of *Spigelia anthelmia* L. (Loganiaceae) were collected from the southern coastal area of Bantul, Yogyakarta, Indonesia (–8.013270, 110.295545) in August 2013 during the transition between the rainy and dry seasons. The plant was taxonomically identified and authenticated at the Department of Pharmaceutical Biology, Faculty of Pharmacy, Universitas Gadjah Mada, Yogyakarta, under the reference letter No. BF2.4/Ident/Det/IX/25, and a voucher specimen (No. 281a) was deposited in the departmental herbarium. After collection, plant material was washed with running tap water, oven-dried at 50 °C for 48 h, and powdered using a mechanical grinder. The resulting powder was stored in airtight containers at room temperature until use.[18]

Chemicals and Reagents

Analytical-grade dichloromethane, n-hexane, methanol, ethyl acetate, chloroform, acetic acid, and silica gel 60 PF_{254} were purchased from Merck (Darmstadt, Germany). Dimethyl sulfoxide (DMSO), sodium dodecyl sulfate (SDS), and potassium dichromate were obtained from Sigma-Aldrich (St. Louis, MO, USA). RPMI-1640 medium, fetal bovine serum (FBS), penicillin–streptomycin, amphotericin B, phosphate-buffered saline (PBS), and trypsin–EDTA were obtained from Gibco (Thermo Fisher Scientific, Waltham, MA, USA). Doxorubicin hydrochloride was purchased from Ebewe Pharma (Unterach, Austria) and used as the positive control in cytotoxicity and apoptosis assays. The Annexin V–FITC/propidium iodide (PI) apoptosis detection kit was obtained from BD Biosciences (San Jose, CA, USA). All other chemicals and reagents were of analytical grade and used without further purification.

Equipment

The following instruments were used in this study: rotary evaporator (Rotavapor R-210, Büchi, Flawil, Switzerland), analytical balance (AUW220D, Shimadzu, Kyoto, Japan), UV cabinet and TLC visualisation system (Camag, Muttenz, Switzerland), CO_2 incubator (HERAcell 150, Thermo Fisher Scientific, Waltham, MA, USA), microplate reader (iMark, Bio-Rad, Hercules, CA, USA), flow cytometer (FACSCalibur, BD Biosciences, San Jose, CA, USA), Fourier-transform infrared (FTIR) spectrophotometer (FTIR 100, PerkinElmer, Waltham, MA, USA), LC–MS system consisting of an HPLC pump (L-6200, Hitachi, Tokyo, Japan) coupled to a Mariner Biospectrometry mass analyser (Applied Biosystems/Sciex, Foster City, CA, USA) with a C18 column (150 mm × 2 mm, 5 µm; Phenomenex, Torrance, CA, USA), and NMR spectrometer (500/125 MHz Delta 2, JEOL, Tokyo, Japan).

Extraction and Partitioning

Powdered plant material (1.2 kg) was extracted with dichloromethane (3 × 5 L) by maceration for 72 h at 25 ± 2 °C with occasional stirring The combined filtrates were filtered and concentrated under reduced pressure at 40 °C using a rotary evaporator to afford the dichloromethane extract. The dried extract was then suspended in methanol and partitioned with an equal volume of n-hexane (n-hexane:methanol, 1:1, v/v) to obtain an n-hexane-soluble phase and a methanol-rich phase. The methanol-rich (n-hexane-insoluble) phase, which showed greater biological activity in preliminary tests, was retained for subsequent bioassay-guided fractionation. All fractions were dried, weighed, and stored at 4 °C until further use.[18]

Bioassay-Guided Fractionation and Isolation

The dichloromethane extract was subjected to vacuum liquid chromatography (VLC) on silica gel 60 PF254 (Merck) using gradient elution with n-hexane, ethyl acetate, and methanol. VLC yielded seven fractions from the dichloromethane extract and four fractions from the chloroform-soluble methanol extract [19]. Fractions were screened for toxicity by the brine shrimp lethality test (BST). The most active fractions were analyzed by thin-layer chromatography (TLC) and purified by preparative TLC (PTLC) with chloroform-methanol (9:1) as the mobile phase. Bioactive bands were collected, yielding Isolate A for subsequent evaluation.[20,21]

Purity Assessment

Chromatographic purity of Isolate A was evaluated by analytical TLC using four solvent systems of different polarity. A single well-defined spot across all systems confirmed purity adequate for cytotoxic and spectroscopic studies.[22,23]

Brine Shrimp Lethality Test (BST)

Toxicity of extracts, fractions, and isolates was assessed using BST.[24,25] Stock solutions were prepared in chloroform–methanol (1:1, v/v), and test concentrations were adjusted to 100 µg/mL in artificial seawater. After solvent evaporation, ten *Artemia salina* nauplii were exposed to each test solution and incubated at 25–27 °C for 24 h. Mortality was recorded at the end of the exposure period. Negative (artificial seawater) and solvent controls were included in each experiment.

Cell Culture and Cytotoxicity Assay (MTT)

Human breast cancer (T47D) and colon cancer (WiDr) cell lines were obtained from a certified culture collection and maintained in RPMI-1640 medium supplemented with 10% fetal bovine serum, 1% penicillin–streptomycin, and 1% amphotericin B at 37 °C in a humidified incubator with 5% CO_2. Cytotoxicity was assessed using the MTT assay.[26] Cells were seeded in 96-well plates at 6×10^3 cells/well and incubated for 24 h. Serial concentrations of Isolate A (12.5–300 µg/mL) were applied for 24 h, with doxorubicin (0.78–100 µg/mL) serving as the positive control. After treatment, 10 µL of MTT solution (5 mg/mL) was added and incubated for 4 h. Formazan crystals were solubilized with 100 µL of 10% SDS in 0.01 N HCl and incubated overnight in the dark. Absorbance was measured at 540 nm using a microplate reader. Cell viability was expressed relative to untreated controls.

Flow Cytometry Assay (Apoptosis Analysis)

Apoptosis was analysed by Annexin V–FITC/propidium iodide (PI) staining as previously described. [27,28] T47D and WiDr cells (1×10^5 cells/well) were seeded in 6-well plates and incubated for 24 h in complete medium. Treatments included Isolate A at 100 µg/mL and doxorubicin at 10 µg/mL as a positive control, while untreated cells and 0.5% DMSO served as negative and vehicle controls, respectively. The concentration of 100 µg/mL for Isolate A was selected as a sub-IC_{50} dose based on the MTT results (approximately 0.6-fold and 0.4-fold of the IC_{50} values for T47D and WiDr cells, respectively), in order to induce a clear apoptotic response while minimizing excessive necrosis. After 24 h of incubation, both floating and adherent cells were harvested, washed twice with cold PBS, resuspended in 1× binding buffer, and stained with Annexin V–FITC (5 µL) and PI (5 µL, 50 µg/mL) for 15 min at 25 ± 2 °C in the dark. Samples were analysed immediately using a BD FACSCalibur flow cytometer (BD Biosciences, San Jose, CA, USA), acquiring at least 10,000 events per sample. Data were processed with FlowJo software (version 10), and Annexin V–FITC versus PI dot plots were divided into four regions: R1 (Annexin V^-/PI^-, viable cells), R2 (Annexin V^+/PI^-, early apoptotic cells), R3 (Annexin V^+/PI^+, late apoptotic or secondary necrotic cells), and R4 (Annexin V^-/PI^+, primary necrotic cells). The percentages of cells in each quadrant were used to quantify the apoptosis profiles reported in the Results and Discussion.

ISSN 2616-0684 (Print)
ISSN 2616-0692 (Electronic)

Spectroscopic Characterization

Isolate A was analysed by Fourier-transform infrared (FTIR) spectroscopy, liquid chromatography–mass spectrometry (LC–MS), and nuclear magnetic resonance (NMR) spectroscopy. FTIR spectra were recorded on a PerkinElmer FTIR 100 spectrophotometer (PerkinElmer, Waltham, MA, USA) using the KBr pellet method over the range 4000–400 cm^{-1}. LC–MS analysis was performed on a Mariner Biospectrometry system coupled to a Hitachi L-6200 LC (Hitachi, Tokyo, Japan) equipped with a Phenomenex C18 column (150 mm × 2 mm, 5 µm; Phenomenex, Torrance, CA, USA). The mobile phase consisted of methanol containing 0.3% acetic acid, delivered isocratically at 0.5 mL/min; the injection volume was 20 µL, and spectra were recorded over m/z 100–1200 in positive electrospray ionisation mode. ^{1}H NMR (500 MHz, DMSO-d_6) and ^{13}C NMR (125 MHz, DMSO-d_6) spectra were obtained on a Delta 2 NMR spectrometer (JEOL, Tokyo, Japan). Chemical shifts (δ) are reported in ppm and were referenced to the residual solvent signals of DMSO-d_6 (δH 2.50 ppm and δC 39.5 ppm). This multimodal spectroscopic approach is standard in natural product research, particularly when the available amount of isolate is limited.[23,29,30]

Statistical Analysis

All experiments were performed in triplicate and data are expressed as mean ± standard deviation (SD). For the BST, LC_{50} values were estimated from plots of log concentration versus corrected percentage mortality using linear regression analysis. For the MTT assay, IC_{50} values were obtained by non-linear regression of log concentration versus cell viability using GraphPad Prism 8. Differences between treatment groups were analysed using one-way ANOVA followed by Tukey's post hoc test or Student's t-test where appropriate, with $p < 0.05$ considered statistically significant. Statistical analyses were performed using SPSS version 25.0 (IBM Corp., Armonk, NY, USA).

Results and Discussion

Bioassay-Guided Isolation and TLC Analysis

Fractionation of the dichloromethane (DCM) extract of Spigelia anthelmia by vacuum liquid chromatography (VLC) on silica gel 60 PF254 using a gradient of n-hexane–ethyl acetate followed by ethyl acetate–methanol afforded seven fractions (I–VII). Thin-layer chromatography (TLC) analysis (Figure 1) showed that fractions I–III were dominated by non-polar spots, whereas fractions VI and VII exhibited more polar bands, with fraction VII displaying the densest pattern of medium-polarity spots. On the basis of these chromatographic profiles, fraction VII was selected for further purification by preparative TLC (PTLC) and subsequent biological evaluation.[19,23]

To link chemical separation with biological activity, all fractions were subjected to the brine shrimp lethality test (BST) at a concentration of 100 µg/mL. The mortality data presented in Table 1 show that Fraction VII exhibited the highest corrected mortality (96%), while Fractions I–VI displayed weak to moderate activity ranging from 4.35% to 43.48%. The control group showed negligible mortality, confirming the specificity of the fractions. This pattern clearly indicates that the most cytotoxic constituents of *S. anthelmia* were concentrated in Fraction VII.

Table 1: Brine shrimp lethality (BST) of VLC fractions (I–VII) of *Spigelia anthelmia* at 100 µg/mL.

Fraction	Corrected % Mortality
Control	0.00
Fraction I	21.74
Fraction II	21.74
Fraction III	8.70
Fraction IV	4.35
Fraction V	43.48
Fraction VI	39.13
Fraction VII	96.00

As summarized in Table 1, Fraction VII displayed the highest corrected mortality in the BST (96.0%), whereas Fractions I–VI showed only weak to moderate lethality, with corrected mortality values below 45%. This result suggests that the bioactive molecules in *S. anthelmia* are predominantly localized in the later-eluting VLC fraction, consistent with moderately polar or semi-polar secondary metabolites.

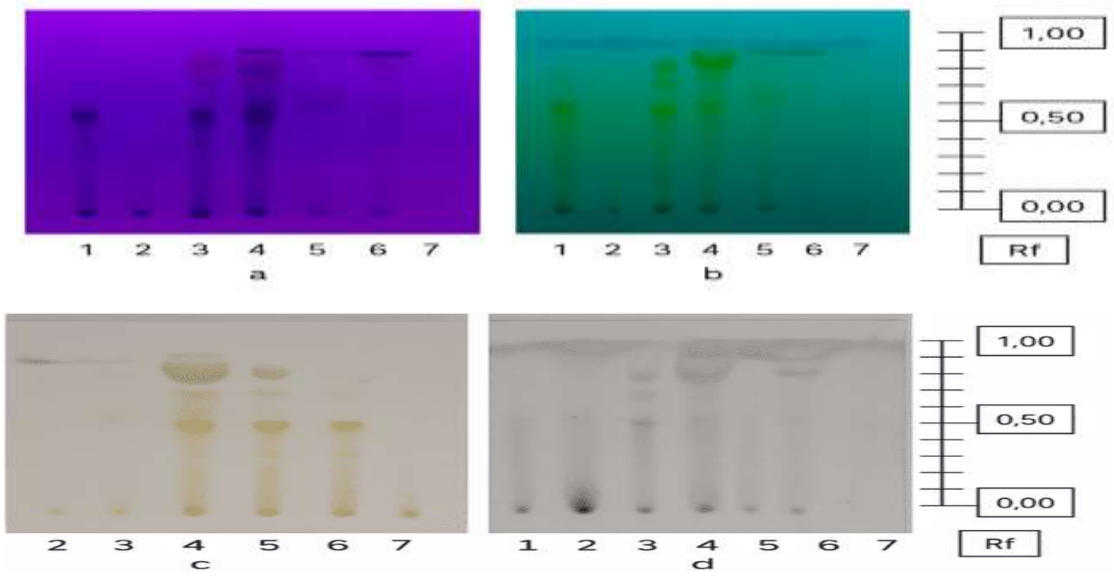

Figure 1: TLC profiles of VLC fractions (I–VII) from the dichloromethane extract of *Spigelia anthelmia* using n-hexane–ethyl acetate (2:1, v/v) as the mobile phase. Plates were visualised under (A) UV 254 nm, (B) UV 366 nm, (C) visible light, and (D) after spraying with cerium sulfate and heating.

ISSN 2616-0684 (Print)
ISSN 2616-0692 (Electronic)

Similar findings have been reported in other toxic medicinal plants, where fractions eluting with intermediate polarity solvents often contain alkaloids, flavonoids, or terpenoids with pronounced biological activities [16,17]. Based on the strong activity of Fraction VII, further purification was carried out using preparative TLC (PTLC). As illustrated in Figure 2, PTLC separation in ethyl acetate solvent successfully resolved Fraction VII into three major bands. Among these, Band 2 with an *R*f value of 0.35 was visually the most intense, suggesting a higher concentration of metabolites. To determine the bioactivity of these separated bands, each was individually evaluated using BST.

The bioassay results are summarized in Table 2, which demonstrate that Band 2 exhibited the highest lethality (92.0 ± 1.15%), followed by Band 1 with moderate activity (52.0 ± 2.10%), while Band 3 showed only weak activity (13.3 ± 1.25%). The remarkably high activity of Band 2 indicates that the principal cytotoxic constituents of *S. anthelmia* were concentrated in this fraction. This active band was therefore designated as Isolate A for subsequent cytotoxicity evaluation in cancer cell lines and spectroscopic characterization.

Table 2: Brine shrimp lethality (BST) of PTLC bands from Fraction VII of *Spigelia anthelmia* at 100 µg/mL.

Band	% Mortality (mean ± SD)
Band 1	52.00 ± 2.10
Band 2	92.00 ± 1.15
Band 3	13.34 ± 1.25

Analytical TLC of Isolate A in four solvent systems of increasing polarity revealed a single, well-defined spot under UV 254/366 nm and after visualisation, indicating the presence of one major component (Figure 3) . Consistently, LC–MS analysis showed a single dominant chromatographic peak at the retention time corresponding to an $[M+H]^+$ ion at m/z 218. These chromatographic and spectrometric features confirm that Isolate A was sufficiently pure for subsequent cytotoxicity testing and spectroscopic characterization.

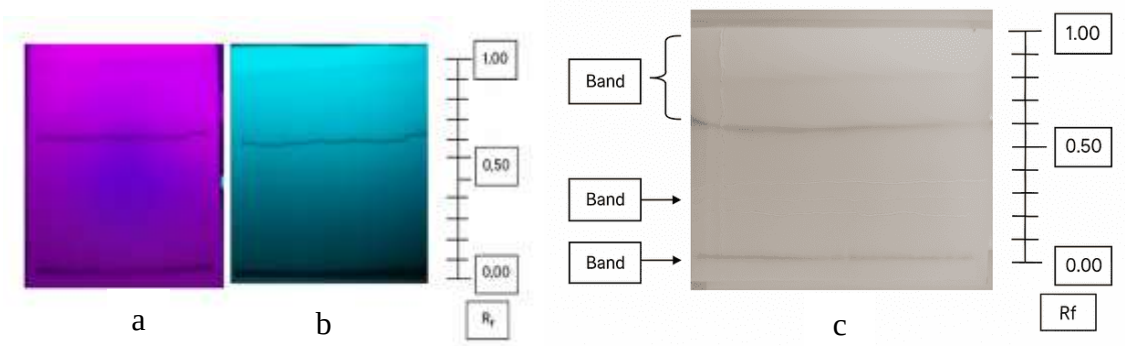

Figure 2: (a–c) PTLC separation of Fraction VII developed in ethyl acetate on silica gel 60 F254, visualized under UV (254 and 366 nm) and after spraying

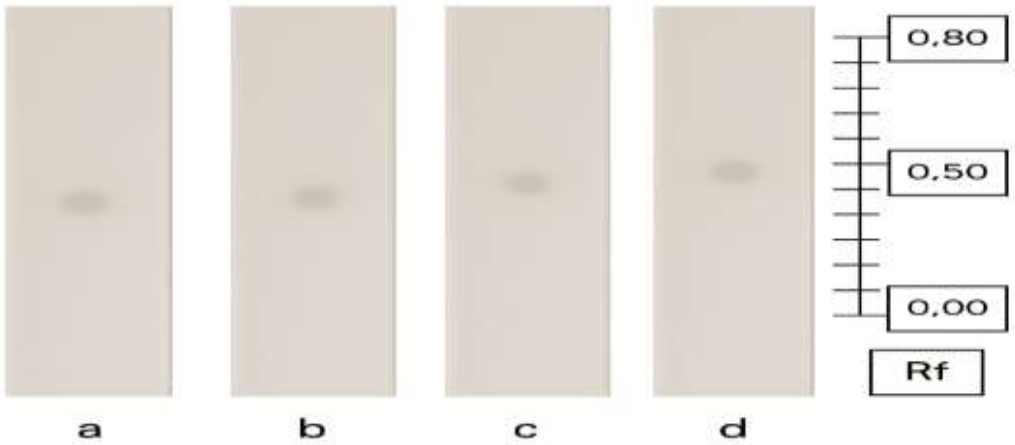

Figure 3: TLC profiles of Isolate A in four solvent systems: (A) n-hexane–ethyl acetate (7:3, v/v), (B) chloroform–methanol (10:1, v/v), (C) dichloromethane–methanol (10:1, v/v), and (D) ethyl acetate–methanol–water (81:11:8, v/v/v). Each plate shows a single well-defined spot, indicating chromatographic purity of the isolate.

The successful isolation of Isolate A through a bioassay-guided approach demonstrates the reliability of combining VLC, PTLC, and BST in identifying active metabolites from complex plant extracts. The use of dichloromethane as an extraction solvent further supports the enrichment of moderately polar metabolites such as alkaloids and terpenoids, which are abundant in *S. anthelmia*.[9,11] Compared to highly polar solvents, dichloromethane provides an optimal balance, extracting compounds that are both pharmacologically active and chemically stable.[18] Collectively, these findings confirm that Fraction VII is the principal bioactive fraction of *S. anthelmia*, and that Isolate A represents a promising candidate for further cytotoxic evaluation and structural elucidation.

Cytotoxic Activity of Isolate A (MTT Assay)

The cytotoxicity of Isolate A was evaluated against breast cancer (T47D) and colon cancer (WiDr) cell lines using the MTT assay. As shown in Figure 5, treatment with Isolate A for 24 h at concentrations between 12.5 and 100 µg/mL produced a concentration-dependent reduction in cell viability in both cell types. One-way ANOVA indicated that the decreases in viability were significant at concentrations ≥ 25 µg/mL compared with untreated controls ($p < 0.05$). Consistent with the descriptive trends in the bar plots, T47D cells were generally more sensitive than WiDr cells, as reflected by lower viability values at corresponding concentrations. Doxorubicin, used as the positive control, caused a much steeper decline in viability across the

ISSN 2616-0684 (Print)
ISSN 2616-0692 (Electronic)

same concentration range, in line with its established potency as a chemotherapeutic agent. Data are expressed as mean ± SD of three independent experiments (n = 3).

The IC_{50} values obtained from regression analysis are summarized in the inset table of Figure 4. Isolate A exhibited IC_{50} values of 166.92 ± 5.10 µg/mL for T47D cells and 245.24 ± 6.25 µg/mL for WiDr cells, whereas doxorubicin showed IC_{50} values of 40.05 ± 2.30 µg/mL and 3.57 ± 0.45 µg/mL, respectively. These numerical values confirm that Isolate A is less potent than doxorubicin but nonetheless displays measurable cytotoxic activity, with a modest preference for T47D breast cancer cells over WiDr colon cancer cells. The overall dose–response relationships for both test compounds are further illustrated in Figure 5, which plots percentage cell viability as a function of concentration. In agreement with the bar charts in Figure 4, the curves show a gradual decline in viability with increasing concentrations of Isolate A, whereas doxorubicin produces a much steeper decrease, particularly in WiDr cells. The sigmoidal shape of the curves is consistent with a typical concentration–response relationship and supports the IC_{50} values obtained from non-linear regression analysis.

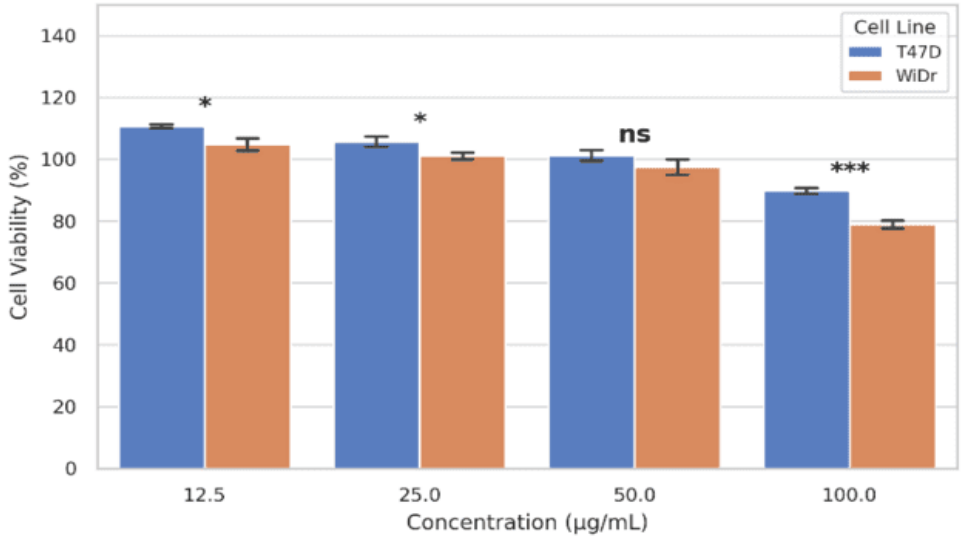

Figure 4: Cytotoxic effects of Isolate A on T47D and WiDr cancer cells after 24 h of treatment at 12.5–100 µg/mL as determined by the MTT assay. Bars represent mean ± SD (n = 3). Statistical differences between cell lines at each concentration were analysed by one-way ANOVA followed by Student's *t*-test ($p < 0.05$, $^{**}p < 0.001$; ns, not significant). The inset table summarises IC_{50} values (mean ± SD) for Isolate A and doxorubicin.

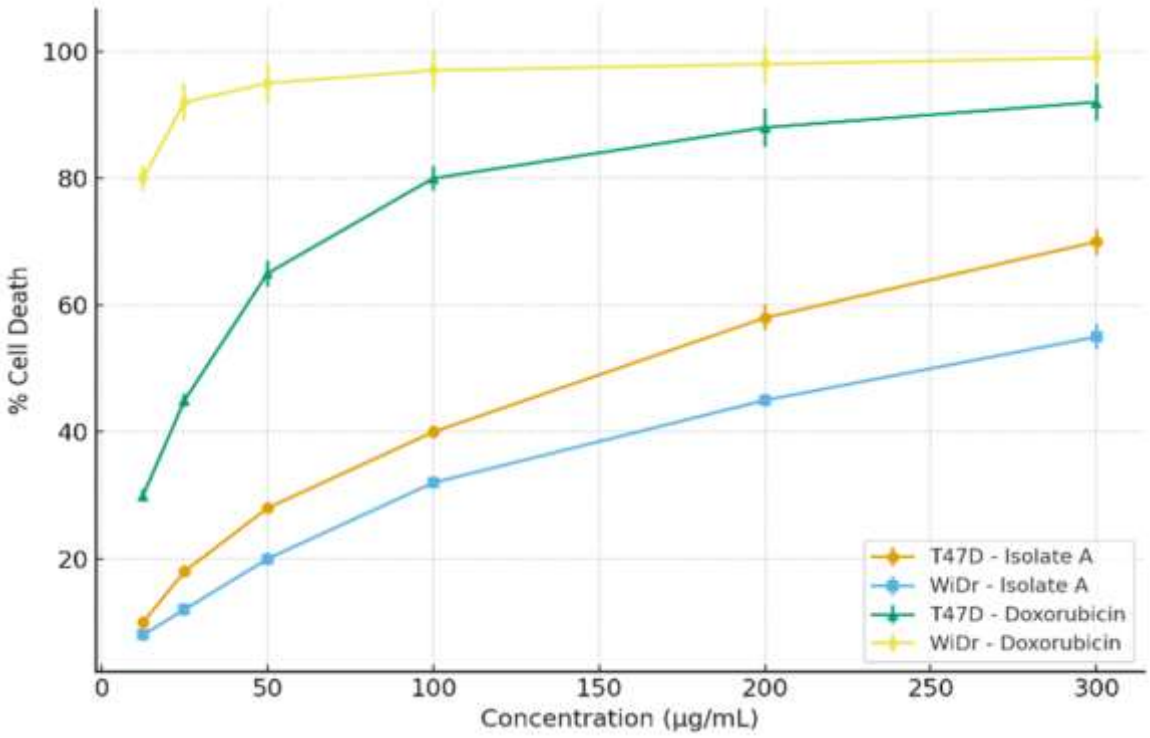

Figure 5: Dose–response curves of Isolate A and doxorubicin against T47D and WiDr cells determined by the MTT assay. Data are expressed as mean ± SD (n = 3).

ISSN 2616-0684 (Print)
ISSN 2616-0692 (Electronic)

The difference in curve slopes underscores two critical observations. First, the steep curve of doxorubicin reflects its high potency but also indicates the potential for severe toxicity. In comparison, the moderate slope of Isolate A suggests a more gradual cytotoxic effect, which could offer advantages in terms of safety if optimized further. Second, the left-shifted curve of T47D relative to WiDr indicates cancer-type selectivity, consistent with previous findings that plant-derived alkaloids and phenolics can exhibit differential cytotoxic responses depending on receptor expression and signaling pathways.[2,31] In addition to apoptosis, several natural alkaloids exert cytotoxicity by interfering with cell cycle progression. For instance, erythraline has been reported to induce G2/M phase arrest in cervical cancer cells through modulation of cyclin B1 and CDK1 expression,[32] while Conofolidine, a bisindole alkaloid, also triggers cell cycle arrest alongside apoptosis by regulating cyclin-dependent kinases and promoting PARP cleavage.[33] Although cell cycle arrest was not specifically evaluated in this study, the gradual dose–response profile observed for Isolate A may suggest a possible contribution of cell cycle modulation in addition to apoptosis.

Collectively, these results demonstrate that Isolate A exerts dose-dependent cytotoxicity through selective inhibition of breast cancer cells, though with lower potency compared to standard chemotherapy. This profile supports its candidacy as a potential lead compound that may be refined structurally or evaluated in combination therapies to improve efficacy.

Apoptosis Induction by Isolate A (Flow Cytometry Analysis)

To clarify whether the cytotoxic effect of Isolate A was associated with apoptosis, T47D and WiDr cells were analysed by Annexin V–FITC/propidium iodide (PI) dual staining followed by flow cytometry. Annexin V–FITC versus PI dot plots were divided into four regions: R1 (Annexin V^-/PI^-, viable cells), R2 (Annexin V^+/PI^-, early apoptotic cells), R3 (Annexin V^+/PI^+, late apoptotic or secondary necrotic cells), and R4 (Annexin V^-/PI^+, primary necrotic cells). The proportions of cells in each quadrant were obtained from the FlowJo gating statistics as the percentage of total acquired events.

Representative plots are shown in Figure 6. In untreated control groups, the vast majority of T47D and WiDr cells were localised in R1, with only a small fraction of events appearing in the apoptotic (R2 and R3) or necrotic (R4) regions. Treatment with Isolate A at 100 µg/mL caused a clear redistribution of cells from R1 into R2 and R3, whereas R4 remained a minor population, indicating that cell death occurred predominantly through apoptosis rather than primary necrosis. In contrast, doxorubicin at 10 µg/mL produced a more pronounced overall apoptotic response, characterised by a higher proportion of cells in R3 and a modest increase in R4, consistent with its established potency as a chemotherapeutic agent. The shift from viable to apoptotic quadrants after exposure to Isolate A was more evident in T47D than in WiDr cells, mirroring the cell-line selectivity observed in the MTT assay.

Taken together, these findings indicate that, under the present experimental conditions, the cytotoxicity of Isolate A in T47D and WiDr cells is mediated mainly through programmed cell death rather than primary necrosis. Similar apoptosis-dominant profiles have been described for several plant-derived alkaloids and phenolic compounds, which frequently induce cancer cell death through caspase activation and perturbation of mitochondrial pathways.[33,34] However, the present study did not assess specific molecular markers such as caspase activity, Bcl-2 family proteins, reactive oxygen species, or mitochondrial membrane potential. Future work should therefore investigate these signalling pathways in order to define more precisely the mechanisms by which Isolate A triggers apoptosis.

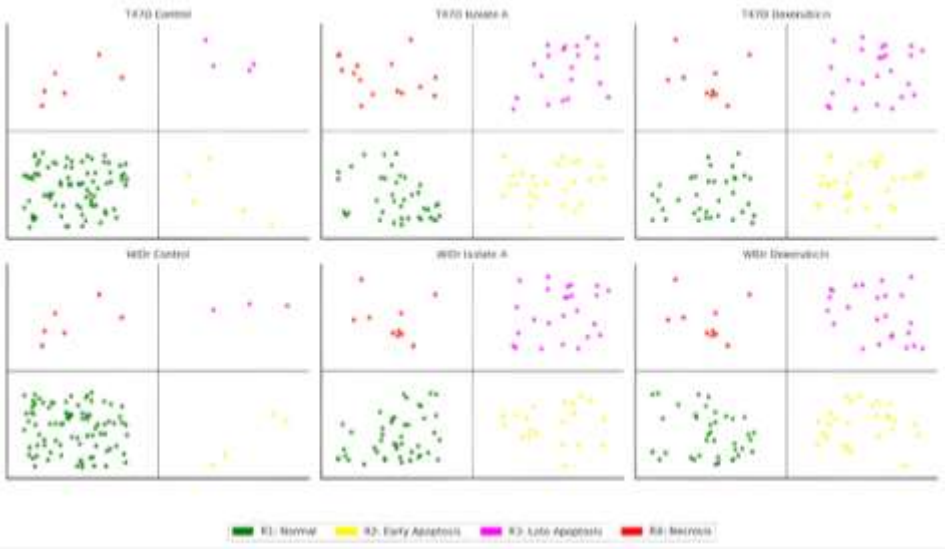

Figure 6: Annexin V–FITC/propidium iodide (PI) flow-cytometry dot plots of T47D and WiDr cells after 24 h treatment with Isolate A (100 µg/mL) or doxorubicin (10 µg/mL) compared with untreated controls. Quadrants denote viable cells (R1, Annexin V^-/PI^-), early apoptotic cells (R2, Annexin V^+/PI^-), late apoptotic or secondary necrotic cells (R3, Annexin V^+/PI^+), and primary necrotic cells (R4, Annexin V^-/PI^+).

Spectroscopic Characterization of Isolate A

The chemical structure of Isolate A was investigated using Fourier-transform infrared (FTIR) spectroscopy, liquid chromatography–mass spectrometry (LC–MS), and nuclear magnetic resonance (NMR) analysis. This combined spectroscopic approach allowed preliminary elucidation of the major functional groups and the overall framework of the isolate. The FTIR spectrum (Figure 7) showed a broad absorption band at 3410 cm^{-1}, consistent with O–H stretching vibrations of hydroxyl groups, together with a sharp band at 1712 cm^{-1} attributable to C=O stretching of a carbonyl moiety (ketone or carboxylic acid). Additional bands in the 1600–1500 cm^{-1} region were assigned to aromatic C=C stretching, while absorptions at 1164–1074 cm^{-1} indicated C–O stretching vibrations. Taken together, these features point to the presence of hydroxyl, carbonyl, and aromatic or heteroaromatic functions, compatible with a phenolic or alkaloid-type framework frequently encountered in medicinal plant metabolites.[23,29]

ISSN 2616-0684 (Print)
ISSN 2616-0692 (Electronic)

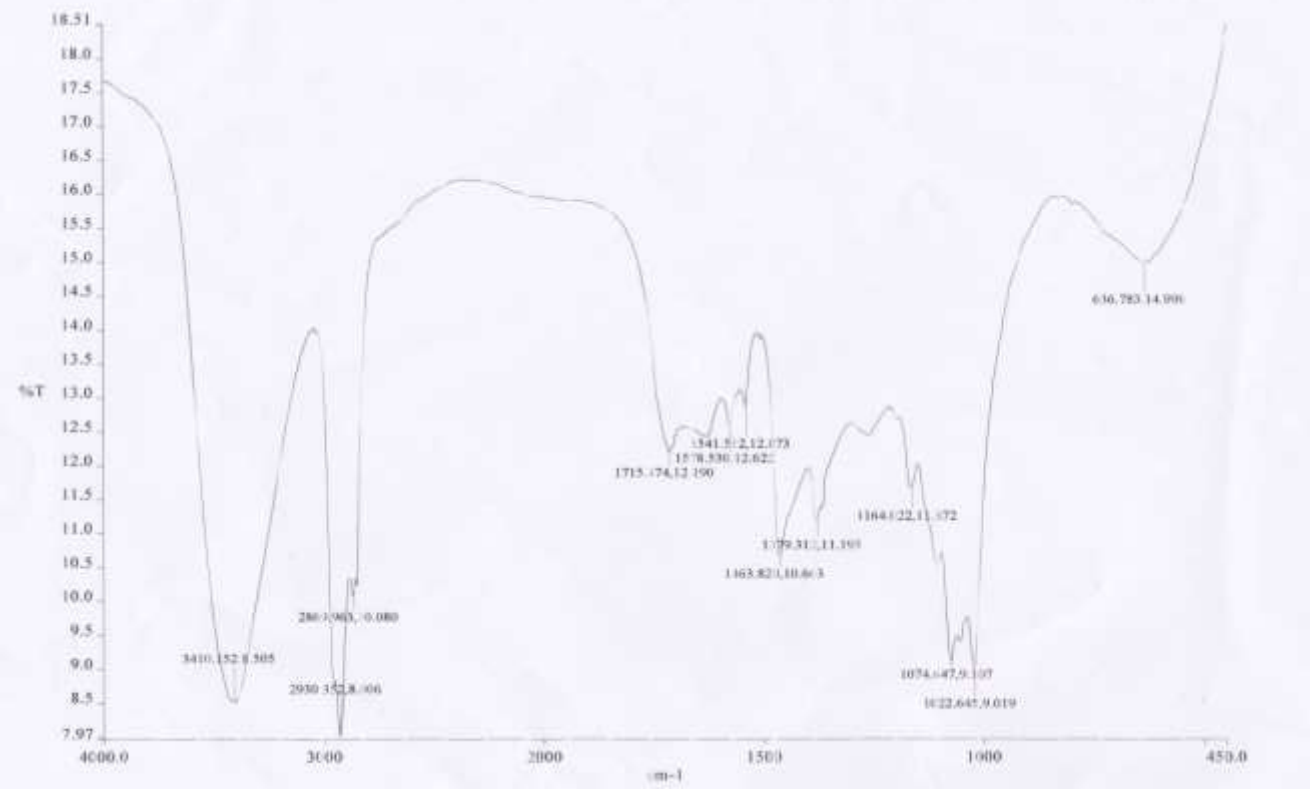

Figure 7: Infrared spectrum of Isolate A (KBr pellet).

LC–MS analysis further supported this interpretation. Isolate A exhibited a single sharp chromatographic peak at 1.85 min, in agreement with the purity assessment described above. The electrospray ionisation (ESI) mass spectrum displayed a dominant protonated molecular ion at m/z 218 $[M+H]^+$, corresponding to an approximate molecular weight of 218 Da, together with fragment ions at m/z 175 and 159 that suggest neutral losses associated with carboxylate and aromatic substituents. While a complete structure could not be established from the available data, the combined FTIR and LC–MS findings indicate a moderately polar phenolic or alkaloid-like scaffold, in line with previous reports of bioactive alkaloids isolated from *S. anthelmia*.[11,35]

Further structural details were obtained from NMR spectroscopy. The ^{1}H NMR spectrum recorded in DMSO-d_6 at 500 MHz displayed a broad singlet at δ 4.8 ppm (phenolic OH), two triplets at δ 3.6 and 3.1 ppm (–CH_2–CH_2–OH groups), and singlets at δ 2.8, 2.6, and 1.1 ppm corresponding to methylene and methyl protons. The ^{13}C NMR spectrum at 125 MHz revealed 16 distinct carbons, including a signal at δ 185 ppm (carbonyl carbon), δ 142–140 ppm (azomethine carbons), δ 121 ppm (nitro-substituted aromatic carbon), and δ 100 ppm (olefinic carbon). These chemical shifts suggest a heteroaromatic framework resembling pyrrole or indole derivatives bearing hydroxyl and carbonyl substituents.

A summary of spectroscopic data and structural interpretation is presented in Table 3. The combined FTIR, LC–MS, and NMR data strongly support that Isolate A is a low-molecular-weight phenolic/alkaloid-type compound (MW ≈ 218 Da) containing hydroxyl, carbonyl, and amine groups, most likely derived from a pyrrole/indole backbone. These chemical signatures resemble previously reported metabolites from *S. anthelmia* and related species, which are known for their anthelmintic and cytotoxic properties.[11,17]

Together, these results highlight that Isolate A is most likely a phenolic alkaloid with structural resemblance to indole or pyrrole derivatives, chemical classes frequently associated with cytotoxic and apoptosis-inducing activities. However, definitive structural confirmation will require advanced methods such as 2D-NMR and high-resolution mass spectrometry.

Table 3: Summary of spectroscopic data and interpretation of Isolate A.

Technique	Observed Data	Structural Assignment
FTIR	3410 cm^{-1}, 1712 cm^{-1}, 1578–1541 cm^{-1}, 1164–1074 cm^{-1}	O–H stretching (phenolic), C=O stretching (carbonyl), N–H bending (amine/amide), C–O stretching
LC–MS	Rt 1.85 min, $[M+H]^+$ at *m/z* 218, fragments at *m/z* 175, 159	MW ≈ 218 Da; fragment losses consistent with carboxylate/aromatic substituents
^{1}H NMR	δ 4.8 (OH, broad s), δ 3.6 & 3.1 (CH_2–CH_2–OH, t), δ 2.8, 2.6, 1.1 (CH_2/CH_3 singlets)	Phenolic OH, aliphatic CH_2 groups, methyl substituents
^{13}C NMR	δ 185 (C=O), δ 142–140 (azomethine C), δ 121 (NO_2-substituted aromatic C), δ 100 (C=C)	Carbonyl, heteroaromatic carbons, nitro/aromatic substitution

Overall Findings and Implications

This study applied a bioassay-guided isolation strategy to identify cytotoxic constituents from *Spigelia anthelmia*. Sequential VLC fractionation and PTLC purification localised the highest brine shrimp lethality to a semi-purified fraction (Isolate A), which exhibited moderate but clear cytotoxic activity against T47D breast and WiDr colon cancer cells. In the MTT assay, Isolate A reduced cell viability in a concentration-dependent manner with IC_{50} values of 166.92 ± 5.10 µg/mL (T47D) and 245.24 ± 6.25 µg/mL (WiDr), whereas doxorubicin, used as a positive control, showed substantially lower IC_{50} values. Although less potent than doxorubicin, Isolate A retained measurable cytotoxicity and showed a modest preference for T47D cells, indicating a degree of cancer-type selectivity.

Flow cytometry with Annexin V–FITC/PI staining demonstrated that Isolate A induces a predominance of Annexin V–positive cell populations, with cells shifting from the viable quadrant into early and late apoptotic quadrants and only a small increase in primary necrosis. This apoptosis-dominant pattern is generally regarded as a desirable feature for anticancer candidates, as it minimises uncontrolled necrotic damage while favouring programmed cell death. The stronger apoptotic response observed in T47D than in WiDr cells is consistent with the differential IC_{50} values and suggests that breast cancer cells may be more susceptible to the active metabolites of *S. anthelmia* under the present experimental conditions.

Spectroscopic analyses provided initial insight into the chemical nature of Isolate A. FTIR bands corresponding to hydroxyl, carbonyl, and aromatic or heteroaromatic functions, together with an $[M+H]^+$ ion at m/z 218 and characteristic fragment ions in the LC–MS spectrum, point to a moderately polar phenolic or alkaloid-like scaffold. These features are in line with previous reports of bioactive alkaloids from *S. anthelmia* and other medicinal plants, although the exact structure of Isolate A could not be fully established due to the limited amount of material available and the absence of complete 2D NMR analysis. Taken together, the biological and spectroscopic data support the view that *S. anthelmia* is a chemically rich species with promising potential as a source of apoptosis-inducing metabolites.

Several limitations of the present work should be acknowledged. The cytotoxicity and apoptosis assays were conducted only in two human cancer cell lines without parallel testing in normal cells, so the selectivity index of Isolate A remains unknown. In addition, the conclusions regarding mechanism are based solely on Annexin V–FITC/PI profiles; no molecular markers such as caspase activation, Bcl-2 family modulation, mitochondrial membrane potential, or reactive oxygen species were measured. Finally, the isolate was obtained in small quantities, precluding more extensive structural studies and in vivo evaluation.

Future investigations should therefore focus on further purification and full structure elucidation of the active constituents, expansion of cytotoxicity testing to a broader panel of cancer and non-transformed cell lines, and mechanistic studies targeting key apoptotic and survival pathways. In vivo assessment in suitable tumour models will also be essential to validate the therapeutic potential of these metabolites. Despite these limitations, the current findings provide a solid foundation for continued exploration of *S. anthelmia* as a natural source of anticancer leads.

Conclusion

In this study, a bioassay-guided isolation strategy was used to identify a semi-purified fraction (Isolate A) from *Spigelia anthelmia* with cytotoxic activity against T47D breast and WiDr colon cancer cells. Isolate A exhibited moderate, concentration-dependent reductions in cell viability and induced an apoptosis-dominant pattern of cell death, as demonstrated by Annexin V–FITC/PI flow cytometry, while spectroscopic data indicated a phenolic or alkaloid-like scaffold. These findings support *S. anthelmia* as a promising natural source of apoptosis-inducing metabolites and provide an initial basis for further anticancer lead discovery.

Conflict of Interest

The authors declare no conflict of interest.

Authors' Declaration

The authors hereby declare that the work presented in this article is original and that any liability for claims relating to the content of this article will be borne by them.

Acknowledgements

The authors gratefully acknowledge the academic support and laboratory facilities provided by the Faculty of Pharmacy, Gadjah Mada University, Indonesia and Faculty of Sports and Health, Gorontalo State University, Indonesia.

References

1. Corsello SM, Nagari RT, Spangler RD, Rossen J, Kocak M, Bryan JG. Discovering the anticancer potential of non-oncology drugs by systematic viability profiling. Nat Cancer. 2020;1(2):235–248. Doi: 10.1038/s43018-019-0018-6.
2. Gezici S, Şekeroğlu N. Current perspectives in the application of medicinal plants against cancer: novel therapeutic agents. Anticancer Agents Med Chem. 2019;19(1):101–111. Doi: 10.2174/1871520619666181224121004.
3. Erb M, Kliebenstein DJ. Plant secondary metabolites as defences, regulators and primary metabolites: the blurred functional trichotomy. Plant Physiol. 2020;184(1):39–52. Doi: 10.1104/pp.20.00433.
4. Pfeffer CM, Singh ATK. Apoptosis: a target for anticancer therapy. Int J Mol Sci. 2018;19(2):448. Doi: 10.3390/ijms19020448.
5. Sung H, Ferlay J, Siegel RL, Laversanne M, Soerjomataram I, Jemal A, Bray F. Global cancer statistics 2020: GLOBOCAN estimates of incidence and mortality worldwide for 36 cancers in 185 countries. CA Cancer J. Clin. 2021; 71(3):209–249. Doi: 10.3322/caac.21660.
6. Huynh QDT, Phan TTT, Liu TW, Duong TLT, Hsu SJ, Kuo CC, Chu MH, Wang YH, Nguyen TV, Shen YA, Fan YJ, Nguyen DK, Vo TH, Lee CK. Cytotoxicity-guided isolation of elatostemanosides I–VI from *Elatostema tenuicaudatum* W.T. Wang and their cytotoxic activities. RSC Adv. 2025; 15(14):10639–10652. Doi: 10.1039/D4RA09007A.
7. Yang J, Hu DB, Xia MY, Luo JF, Li XY, Wang YH. Bioassay-guided isolation of cytotoxic constituents from the flowers of *Aquilaria sinensis*. Nat Prod Bioprospect. 2022;12(1):11. Doi: 10.1007/s13659-022-00334-3.
8. Chen L, Liu Y, Li Y, Yin W, Cheng Y. Anti-cancer effect of sesquiterpene and triterpenoids from agarwood of *Aquilaria sinensis*. Molecules. 2022;27(16):5350. Doi: 10.3390/molecules27165350.
9. Van Wyk AS, Prinsloo G. Health, safety and quality concerns of plant-based traditional medicines and herbal remedies: a review. S Afr J Bot. 2020;133:54–62. Doi: 10.1016/j.sajb.2020.06.017.
10. Nelson LS, Shih RD, Balick MJ, Lampe KF. Handbook of Poisonous and Injurious Plants. 2nd ed. New York: Springer; 2007. p. 21-34.
11. Akbar S. Handbook of 200 Medicinal Plants: A Comprehensive Review of Their Traditional Medical Uses and Scientific Justifications. Springer; 2020.
12. Raszewski JA, Sharma S. Physiology, ryanodine receptor. In: StatPearls. Treasure Island (FL): StatPearls Publishing; 2022.
13. Taupik M, Suryadi AMA, La Kilo J, Uno WZ, Badjeber SB. Identification of secondary metabolite compounds in leaves of *Spigelia anthelmia* L. and antioxidant activity using the DPPH (1,1-diphenyl-2-picrylhydrazyl) method. J Syifa Sci Clin Res. 2022;4(3):694–708. Doi:10.37311/jsscr.v4i3.15927.
14. Danlami U, Cecilia OE, Ifeanyi OM. Evaluation of the phytochemicals and antimicrobial activities of the ethanolic,

hexane and ethyl acetate extracts of *Spigelia anthelmia* leaves. Int J Pharm Chem. 2017;3(3):29–35.
15. Ukwade CE, Ebuehi OAT, Adisa RA. Phytochemical and cytotoxic screening of selected medicinal plants (*Byrsocarpus coccineus*, *Terminalia avicennioides* and *Anogeissus leiocarpus*) using brine shrimp (*Artemia salina*) lethality assay. Eur J Nutr Food Saf. 2020;12(4):60–71.
16. Assis LM, Bevilaqua CML, Morais SM, Vieira LS, Costa CTC, Souza JAL. Ovicidal and larvicidal activity in vitro of *Spigelia anthelmia* Linn. extracts on *Haemonchus contortus*. Vet Parasitol. 2003;117(1):43–49.
17. Ribeiro WLC, Andre WPP, Cavalcante GS, de Araújo-Filho JV, Santos JML, Macedo ITF, de Melo JV, de Morais SM, Bevilaqua CML. Effects of *Spigelia anthelmia* decoction on sheep gastrointestinal nematodes. Small Rumin. Res. 2017; 153:146–152. Doi: 10.1016/j.smallrumres.2017.06.001.
18. Chibuye B, Indra SS, Luke C, Kakoma MK. A review of modern and conventional extraction techniques and their applications for extracting phytochemicals from plants. Sci Afr. 2023;19:e01585. Doi:10.1016/j.sciaf.2022.e01585.
19. Coll JC, Bowden BF. The application of vacuum liquid chromatography to the separation of terpene mixtures. J Nat Prod. 1986;49(5):934–936.
20. Sonam M, Singh RP, Pooja S. Phytochemical screening and TLC profiling of various extracts of *Reinwardtia indica*. Int J Pharmacogn Phytochem Res. 2017;9(4):523–527.
21. Arung ET, Wicaksono BD, Handoko YA, Kusuma IW, Yulia D, Sandra F. Anti-cancer properties of diethyl ether extract of wood from sukun (*Artocarpus altilis*) in human breast cancer (T47D) cells. Trop J Pharm Res. 2009;8(4):317–324.
22. Sarker SD, Nahar L. An introduction to natural products isolation. In: Sarker SD, Nahar L, editors. *Natural Products Isolation.* Totowa (NJ): Humana Press; 2012. p. 1–25.
23. Wagner H, Bauer R, Melchart D, Xiao PG, Staudinger A, editors. Chromatographic Fingerprint Analysis of Herbal Medicines. Vol. III: Thin-Layer and High-Performance Liquid Chromatography of Chinese Drugs. Cham: Springer; 2015.
24. Ogbole OO, Ndabai NC, Akinleye TE, Attah AF. Evaluation of peptide-rich root extracts of *Calliandra portoricensis* (Jacq.) Benth (Mimosaceae) for in vitro antimicrobial activity and brine shrimp lethality. BMC Complement Med Ther. 2020;20(1):1–7. Doi: 10.1186/s12906-020-2836-6.
25. Wulandari DD, Risthanti RR, Sari EAP, Anisa H, Filia S. Phytochemical screening and toxicological evaluation using brine shrimp lethality test of ethanolic extract of *Morinda citrifolia* L. Bali Med J. 2022;11(2):561–565. Doi: 10.15562/bmj.v11i2.3119.
26. Hayaza S, Wahyuningsih SPA, Susilo RJK, Permanasari AA, Husen SA, Winarni D. Anticancer activity of okra raw polysaccharides extracts against human liver cancer cells. Trop J Pharm Res. 2019;18(8):1667–1672.
27. Ifora I, Hamidi D, Susanti M, Wahyuni FS. Dual-method apoptosis evaluation reveals the therapeutic potential of *Garcinia cowa* extract in combination with doxorubicin for breast cancer treatment. Trop J Nat Prod Res. 2025;9(7):3076–3081. Doi:10.26538/tjnpr/v9i7.18.
28. Alshehade SA, Almoustafa HA, Alshawsh MA, Chik Z. Flow cytometry-based quantitative analysis of cellular protein expression in apoptosis subpopulations: a protocol. Heliyon. 2024;10(13):e33665. Doi: 10.1016/j.heliyon.2024.e33665.
29. Cocan I, Alexa E, Danciu C, Radulov I, Galuscan A, Obistioiu D, Morvay AA, Sumalan RM, Poiana MA, Pop G, Dehelean CA. Phytochemical screening and biological activity of Lamiaceae family plant extracts. Exp Ther Med. 2018; 15(2):1863–1870. Doi: 10.3892/etm.2017.5640.
30. Rabel F, Sherma J. Review of the state of the art of preparative thin-layer chromatography. J Liq Chromatogr Relat Technol. 2017;40(4):165–176.
31. Mahmoud AM, Hernández Bautista RJ, Sandhu MA, Hussein OE. Beneficial effects of citrus flavonoids on cardiovascular and metabolic health. Oxid Med Cell Longev. 2019;2019:1–19.
32. Miranda CAN, Souza ATB de, Soares AKM da C, Bernardes-Oliveira E, Rocha HAO, Barbosa EG. Apoptosis and G2/M Phase Cell Cycle Arrest Induced by Alkaloid Erythraline Isolated from Erythrina velutina in SiHa Cervical Cancer Cell. Int J Mol Sci. 2025;26(10):4627. Doi: 10.3390/ijms26104627.
33. Al-Hayali MZ, Nge CE, Lim KH, Collins HM, Kam TS, Bradshaw TD. Conofolidine: a natural plant alkaloid that causes apoptosis and senescence in cancer cells. Molecules. 2024;29(11):2654.
34. Calaf GM, Crispin LA, Quisbert-Valenzuela EO. Noscapine and apoptosis in breast and other cancers. Int J Mol Sci. 2024;25(6):3536.
35. Ghisalberti EL. Detection and isolation of bioactive natural products. In: Atta-ur-Rahman, editor. *Bioactive Natural Products.* Boca Raton (FL): CRC Press; 2007. p. 25–90.